Available online at www.sciencedirect.com
SCIENCE DIRECT®
Journal of Molecular Catalysis A: Chemical 208 (2004) 267–271
JOURNAL OF MOLECULAR CATALYSIS A: CHEMICAL
www.elsevier.com/locate/molcata

Effects of zirconia phase on the synthesis of higher alcohols over zirconia and modified zirconia

Daiping He, Yunjie Ding*, Hongyuan Luo, Can Li

Natural Gas Utilization and Applied Catalysis Laboratory, Dalian Institute of Chemical Physics, Chinese Academy of Sciences, Dalian 116023, China

Received 3 June 2003; received in revised form 29 July 2003; accepted 31 July 2003

Abstract

The catalytic performances of ZrO_2-based catalysts were evaluated for the synthesis of higher alcohols from synthesis gas. The crystal phase structures were characterized by X-ray diffraction (XRD) and UV Raman. The results indicated that ZrO_2 and Pd modified ZrO_2 catalysts were effective catalysts in the synthesis of ethanol or isobutanol, and their selectivities basically depended on the crystal phase of ZrO_2 surface. The ZrO_2 with surface tetragonal crystal phase exhibited a high activity to form ethanol, while the ZrO_2 with surface monoclinic crystal phase exhibited a high activity to form isobutanol. Temperature-programmed desorption (TPD) experiment indicated that the high activity of isobutanol formation from synthesis gas over monoclinic zirconia was due probably to the strong Lewis acidity of Zr^{4+} cations and the strong Lewis basicity of O^{2-} anions of coordinative unsaturated Zr^{4+}–O^{2-} pairs on the surface of monoclinic ZrO_2.

Keywords: Higher alcohol synthesis; Synthesis gas; Zirconia; Crystal phase

1. Introduction

Over the last 20 years, the synthesis of higher alcohols from mixtures of H_2 and CO (syngas) has drawn considerable interest due to the increasing demand for octane boosters, which do not cause any environmental problems, especially isobutanol, which represents a potential gasoline additive and a precursor for obtaining isobutene, in turn converted to methyl tert-butyl ether (MTBE) or to isooctane (via isobutene dimerization and successive hydrogenation) when MTBE will be no more desired as gasoline additive, as for example in California. Several isobutanol synthesis catalytic systems have been investigated in recent years. Typical isobutanol yields reported in the literature are shown in Table 1. The Pd promoted zirconia mixed oxides was found to be an effective catalyst for the direct synthesis of isobutanol from synthesis gas. Though extensive studies on zirconia-based catalysts have been made, such as the effects of catalyst composition, various promoters and reaction conditions etc. on isobutanol formation [6–11], the relationship between isobutanol formation and the crystal phase structure of ZrO_2 has hardly been studied.

Zirconia exhibits three different phases: monoclinic (m-ZrO_2), tetragonal (t-ZrO_2) and cubic (c-ZrO_2). The phase structure of zirconia is important for many materials and catalytic reactions, for example, stabilized *tetragonal* zirconia is considered an important structure for ceramics because of its excellent mechanical properties such as fracture toughness, strength, and hardness. However, a phase transformation from tetragonal phase to the monoclinic phase of crystalline ZrO_2 prevents its applications from a broader temperature ranges. Bell and coworkers [12] recently reported that zirconia-supported copper catalysts exhibit a high activity for synthesis of methanol from both CO/H_2 and CO_2/H_2, and the catalyst prepared on m-ZrO_2 was 4.5 times more active for methanol synthesis from CO_2/H_2 than that prepared on t-ZrO_2, and 7.5 times more active when CO/H_2 was used as the feed. The adsorption of CO and CO_2 on tetragonal and monoclinic ZrO_2 have been carried out using infrared spectroscopy (IR) and temperature-programmed desorption (TPD) [13,14]. The CO_2 adsorption capacity of m-ZrO_2 is more than an order of magnitude higher than that of t-ZrO_2. The CO adsorption capacity of m-ZrO_2 is 5- to 10-fold higher than that

* Corresponding author. Tel.: +86-411-4379143; fax: +86-411-4379143.
E-mail address: dyj@dicp.ac.cn (Y. Ding).

1381-1169/$ – see front matter © 2003 Elsevier B.V. All rights reserved.
doi:10.1016/S1381-1169(03)00542-9

Table 1
Representative isobutanol synthesis catalysts

Catalyst	T (K)	P (Mpa)	CO/H_2	GHSV (h^{-1})	Isobutanol yield ($g/l_{cat}/h$)
Cu-Mg-Ce-K [1]	593	5.1	1.0/1.0	1832	7.2[a]
Zn-Cr-K [2]	693	32.5	1.0/2.2	15000	125
Cu-Zn-Mn-Co-Cr-K-Cs [3]	683	17.5	1.0/2.0	40000	358
Cu-Zn-Cr-Cs [4]	583	9.1	1.0/0.45	5330	51
Cu-Zn-Mn-K [5]	643	10.0	0.5/1.0	10000	175
Pd-Zr-Zn-Mn-K [6]	693	25.0	1.0/1.0	20000	740

[a] $g/kg_{cat}/h$.

of t-ZrO_2. Infrared spectroscopy has revealed the presence of three types of hydroxyl groups on ZrO_2: terminal, bi-bridged, and tri-bridged. These studies have motivated efforts aimed at understanding the effects of the crystal phase structure of ZrO_2 on isobutanol formation.

In this paper, the catalytic performances of CO hydrogenation to higher alcohols over ZrO_2-based catalysts are investigated. The crystal phase structures of ZrO_2 are measured, and the relationship between isobutanol formation and the crystal phase structures of ZrO_2 is discussed on the basis of the observed surface properties.

2. Experimental

Hydrous zirconia (ZrO_2 precursor) was prepared from zirconium nitrate with sodium hydroxide at 273 K, keeping the pH constant at 11.0. Two kinds of zirconia (ZrO_2-a and ZrO_2-b) were prepared from this precursor. ZrO_2-a was prepared by washing the precursor twice, and ZrO_2-b four times, drying at 383 K for 10 h, and then calcining at 873 K for 4 h. Preparation of promoted ZrO_2 catalysts was conducted as follows: a solution of Li and Pd nitrates was concurrently impregnated on ZrO_2. The loadings of Li and Pd were 7.5 and 1.0 mol% on a metals basis only, respectively. The resulted material was dried at 383 K for 10 h followed by 3 h of calcination at 573 K.

The CO hydrogenation reaction over ZrO_2-based catalysts (1 g) was carried out under conditions: H_2:CO = 2 (volume ratio), 673 K, 8.0 MPa, and 15000 h^{-1} in a conventional flow reactor. The effluent passed through a condenser filled with 100 ml of cold de-ionic water. The formed oxygenates were completely captured by dissolution into the water. The aqueous solution containing oxygenates was analyzed by off-line HP4890 gas chromatography with a PEG capillary column and FID as detector using 1-pentanol as an internal standard. The tail gas was analyzed by on-line HP 4890 GC with a Porapak QS column and TCD as detector.

X-ray diffraction of zirconia was determined by an X-ray diffractometer (D/Max-γB, Rigaku) operating at 40 kV and 200 mA using Cu Kα radiation. UV Raman spectra were recorded on a homemade UV Raman spectrograph, which has four main parts: an UV cw laser, a Spex 1877d triplemate spectrograph, a CCD detector, and an optical collection system. The 244 nm line from Innova 300 FRED was used as the excitation source. The laser power of the 244 nm line at the samples was below 2.0 mw. The specific surface area of zirconia was determined from nitrogen adsorption–desorption isotherms at liquid nitrogen temperature on a Micromeritics ASAP-2010 instrument. CO_2-TPD test was carried out in a flow apparatus made by Micromeritics (Model Autochem 2910). The sample (0.2 g) was treated at its calcined temperature in helium flow for 1 h. After cooling to 323 K, the sample was saturated with CO_2. After this purging treatment, the sample was heated to 773 K at 10 K/min in a helium flow of 40 cm^3/min. The desorpted CO_2 was analyzed by an on-line TCD.

3. Results and discussion

The catalytic results obtained over ZrO_2-based catalysts at 673 K, 8.0 MPa, 15000 h^{-1} are presented in Table 2. The results show that ZrO_2 can catalyze CO hydrogenation to higher alcohols. Li- and Pd-promoted ZrO_2 catalysts significantly improved the activity of ZrO_2 for the synthesis of higher alcohols. The space time yield (STY) of alcohols over

Table 2
The catalytic properties of ZrO_2-based catalysts

Catalyst	CO conv (%)	Selectivity (C mol%)				STY[a] (alcohol)	Alcohol distribution (wt.%)				
		C_xH_y	CO_2	ROH	DME[b]	$g/kg_{cat}\,h$	C_1	C_2	C_3	I-C_4	Others[c]
ZrO_2-a	1.85	33.3	50.1	16.6	0	8.3	90.1	6.4	1.2	2.3	0
ZrO_2-a[d]	8.43	35.4	29.8	34.3	0.5	214.9	66.6	25.1	6.2	1.3	0.8
ZrO_2-b	2.54	31.9	20.1	43.7	4.3	29.6	91.5	0	0	8.5	0
ZrO_2-b[e]	7.78	35.6	17.5	46.6	0.3	146.3	73.7	0.8	0.6	23.1	1.8

Reaction conditions: $T = 673$ K, $P = 8.0$ MPa, GHSV = 15000 h^{-1}.
[a] STY: space time yield.
[b] DME: dimethyl ether.
[c] Others: C_{4+} OH.
[d] ZrO_2-a: Li-Pd-ZrO_2-a.
[e] ZrO_2-b: Li-Pd-ZrO_2-b.

Table 3
Chemical composition and BET surface areas of ZrO_2-based catalysts

Catalyst	Composition analysis (mol%)[a]				S_{BET} (m^2/g)
	Zr	Na	Li	Pd	
ZrO_2-a	91.8	8.2	0	0	30
Li-Pd-ZrO_2-a	83.9	7.5	7.6	1.0	23
ZrO_2-b	96.9	3.1	0	0	32
Li-Pd-ZrO_2-b	88.3	2.8	7.9	1.0	27

[a] Calculated as metals from X-ray fluorescence (XRF).

ZrO_2-a increased dramatically from 8.3 up to 214.9 g/kg_{cat} h, and the selectivity of ethanol increased from 6.4 up to 25.1% when Li and Pd were added into ZrO_2-a catalyst. Similar promoting effects of Li and Pd were observed in the case of ZrO_2-b catalyst. The selectivity of isobutanol was up to 23.1%. It was interesting to note that both ZrO_2-a and Li, Pd promoted ZrO_2-a catalysts exhibited a high selectivity towards ethanol, while both ZrO_2-b and Li, Pd promoted ZrO_2-b catalysts exhibited a high selectivity towards isobutanol, only a little ethanol was detected in the alcohols fraction.

Table 3 shows the chemical composition and BET surface areas of ZrO_2-based catalysts studied here. Besides zirconia, ZrO_2-a and ZrO_2-b contained 8.2 and 3.1 mol% (on a metals basis only) of sodium, respectively. The BET surface areas of ZrO_2-a and ZrO_2-b were almost the same. The decrease in the surface area was observed when Li and Pd were added into ZrO_2-a and ZrO_2-b.

Fig. 1 shows the XRD patterns of ZrO_2-a, Li-Pd-ZrO_2-a, ZrO_2-b and Li-Pd-ZrO_2-b catalysts. The "t" and "m" in the figure denote the tetragonal and monoclinic phases, respectively. The diffraction peaks of only tetragonal phase were found in the ZrO_2-a and Li-Pd-ZrO_2-a. Mixture phases of monoclinic and tetragonal were observed in the ZrO_2-b and Li-Pd-ZrO_2-b.

Fig. 2 displays the UV Raman spectra of ZrO_2-a, Li-Pd-ZrO_2-a, ZrO_2-b and Li-Pd-ZrO_2-b catalysts. It can be seen in the Raman spectrum that the major bands are at 259, 312, 472 and 640 cm^{-1} which are assigned to the tetragonal phase of ZrO_2 [15–17] for the ZrO_2-a catalyst. While

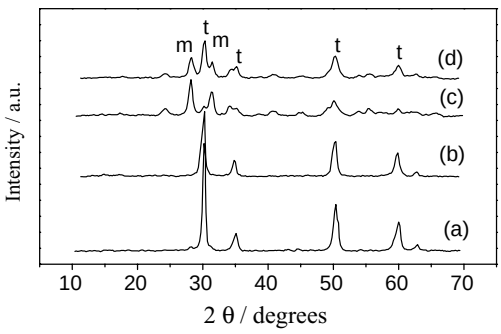

Fig. 1. X-ray diffraction patterns of (a) Li-Pd-ZrO_2-a, (b) ZrO_2-a, (c) Li-Pd-ZrO_2-b, and (d) ZrO_2-b catalysts.

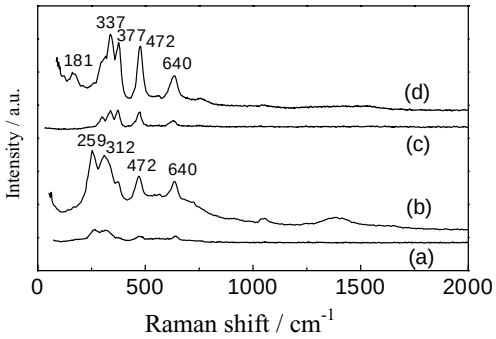

Fig. 2. UV Raman Spectra of (a) Li-Pd-ZrO_2-a, (b) ZrO_2-a, (c) Li-Pd-ZrO_2-b, and (d) ZrO_2-b catalysts.

the bands at 181, 337, 377, 472 and 640 cm^{-1}, assigned to monoclinic zirconia [15–17] can be observed on the ZrO_2-b catalyst. The intensity of Li- and Pd-promoted ZrO_2-a and ZrO_2-b catalysts decreased substantially compared with those obtained from ZrO_2-a and ZrO_2-b catalysts. Several factors can contribute to this decrease, i.e. the Raman spectra were adsorbed and scattered by the promoters added on ZrO_2-a and ZrO_2-b catalysts. It is obvious, from the combination of XRD patterns and UV Raman spectra, that there is tetragonal phase in the bulk and the surface of ZrO_2-a and Li-Pd-ZrO_2-a catalysts, and tetragonal and monoclinic phases in the bulk and monoclinic phase on the surface of ZrO_2-b and Li-Pd-ZrO_2-b catalysts.

Zirconia exists in three different phases: monoclinic, tetragonal and cubic. Many studies have addressed the factors that affect the phase transformation of tetragonal zirconia, such as the amount of stabilizer [18,19], the pH values of precipitation in the synthesis [14,20], the grain size of the tetragonal powder [21,22] etc., and it has been found that zirconia changes from tetrogonal to monoclinic phase with calcination temperature elevated and the phase transition takes place initially at the surface regions [15] and the phase change from tetrogonal to monoclinic is significantly prevented by the incorporation of Y, La, K, Na [23,24] etc. On the basis of the results reported in the literature, we supposed that the difference of the surface phase of ZrO_2-a and ZrO_2-b in this study probably resulted from the Na incorporated into zirconia, which retarded the phase change of tetragonal to monoclinic ZrO_2 during calcination.

Table 4 shows how adding methanol, 1-propanol into the feed influences alcohol distribution and productivity. Addition of 1-propanol or methanol increased the formation of isobutanol. Nevertheless, the addition of 1-propanol favored isobutanol formation, and the 1-propanol added into the feed was nearly completely converted into Isobutanol, 2-methylbutanol-1, 2-methylpentanol-1 and 2-ethylbutanol-1.

The results presented above show that the mechanism for the formation of isobutanol on Li-Pd-ZrO_2-b catalyst is identical with that in the literature. The most accepted reaction

Table 4
Effect of methanol and 1-propanol added into feed on product composition

Product, STY ($g/kg_{cat}\,h$)	Alcohol added		
	None	Methanol	1-Propanol
Methanol	107.8	–	94.8
Ethanol	1.2	1.7	2.0
1-Propanol	0.8	1.3	–
Isobutanol	33.8	39.7	58.2
2-Methylbutanol-1	0.9	1.9	2.4
2-Methylpentanol-1	1.8	2.3	4.8
2-Ethylbutanol-1	0	1.7	3.4

Catalyst: Li-Pd-ZrO_2-b, $H_2/CO = 2$, $T = 673\,K$, $P = 8.0\,MPa$, GHSV = $15000\,h^{-1}$. Alcohol added: methanol, 3.12 mmol C/h; 1-propanol, 1.26 mmol C/h.

network for higher alcohol synthesis given by Klier et al. [25] for cesium promoted Cu/Zn-oxide catalysts describes the mechanistic differences between the reaction paths to methanol and isobutanol. The first step in higher alcohol synthesis is hydrogenation of CO to a surface intermediate which is similar to methanol. Linear primary alcohols are built by linear chain growth including CO insertion steps. Isobutanol and 2-methybutanol-1 originate from β-addition including aldolic condensation. Formation of 1-propanol can be reached via both pathways (Scheme 1). Isobutanol do not undergo consecutive reactions following this network, due to its high steric hindrance and to the presence of only one hydrogen in α-position to the methylol group. The chain growth occurs by aldolic condensation with hydrogen loss at α-position or β-position carbon atom, the latter being the faster process. It was also assumed that hydrogen loss from methanol slower than from a β-carbon. Thus the methanol and isobutanol were the major products in the alcohol fraction.

CO_2-TPD spectra of ZrO_2-a, Li-Pd-ZrO_2-a, ZrO_2-b and Li-Pd-ZrO_2-b catalysts are shown in Fig. 3. It is evident that the CO_2 adsorption capacity of ZrO_2-b is significantly higher than that of ZrO_2-a, and the strength of CO_2 adsorption is stronger on ZrO_2-b. Consistent with the present findings, it has been reported that the CO_2 adsorption capacity of m-ZrO_2 is more than an order magnitude higher than that of t-ZrO_2 by Bell and coworker [13]. They suggested that the high CO_2 adsorption capacity of m-ZrO_2 is attributed to the high concentration and basicity of the hydroxyl groups on this polymorph, as well as the strong Lewis acidity of

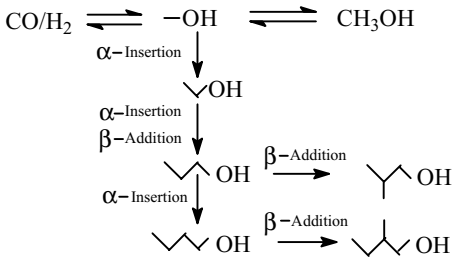

Scheme 1. Reaction network for alcohol synthesis from CO/H_2.

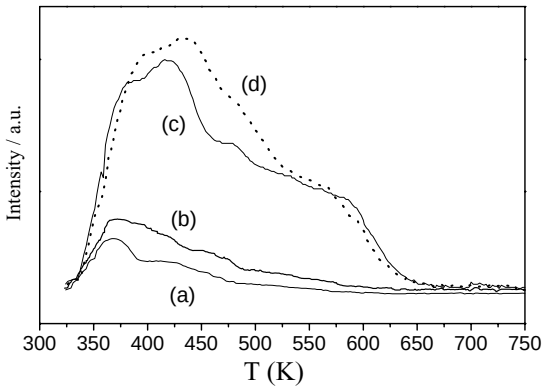

Fig. 3. CO_2-TPD on (a) ZrO_2-a, (b) Li-Pd-ZrO_2-a, (c) ZrO_2-b, and (d) Li-Pd-ZrO_2-b catalysts.

Zr^{4+} cations and the strong Lewis basicity of O^{2-} anions of coordinative unsaturated Zr^{4+}–O^{2-} pairs on the surface of m-ZrO_2. The shape and position of TPD spectra of CO_2 from Li- and-Pd promoted ZrO_2-a and ZrO_2-b are similar to that from ZrO_2-a and ZrO_2-b seen in Fig. 3. The difference is that CO_2 adsorption capacity somewhat increases when Li and Pd are added into ZrO_2-a and ZrO_2-b.

The surface requirements for the two isosynthesis chain growth reactions, condensation and CO insertion over zirconium dioxide were studied by Jackson et al. [26]. Lewis acid sites and oxygen vacancies were found to enhance the condensation reaction. The CO insertion reaction was enhanced by basic sites. The selectivity of the isosynthesis reaction is caused by a balance between the strength and quantity of acid and base sites on zirconia. Thus the high isobutanol selectivity on ZrO_2-b is due probably to the strong Lewis acidity of Zr^{4+} cations and the strong Lewis basicity of O^{2-} anions of coordinative unsaturated Zr^{4+}–O^{2-} pairs on the surface of ZrO_2-b, which enhance the isosynthesis chain growth reactions, CO insertion and aldolic condensation in the isobutanol formation.

4. Conclusion

Based on the above outcomes, we can conclude that the crystal phase of ZrO_2 surface may play an important role in selectivities toward ethanol or isobutanol. The tetragonal phase on the surface region of ZrO_2-a and Li, Pd promoted ZrO_2-a catalysts may be responsible for the high selectivity towards ethanol, while the monoclinic phase on the surface of ZrO_2-b and Li, Pd promoted ZrO_2-b catalysts may be crucial to the high isobutanol selectivity. The high isobutanol selectivity on ZrO_2-b is due probably to the stronger Lewis acidity of Zr^{4+} cations and the stronger Lewis basicity of O^{2-} anions of coordinative unsaturated Zr^{4+}–O^{2-} pairs on the surface of ZrO_2-b, which enhance the isosynthesis chain growth reactions, CO insertion and aldolic condensation in the isobutanol formation.

Acknowledgements

This work was financially supported by the Innovation Funding of the Chinese Academy of Sciences (KGCX2-302-01).

References

[1] C.R. Apesteguia, B. DeRites, S. Soled, Catal. Lett. 44 (1997) 1.
[2] W.S. Epling, G.B. Hoflund, W.M. Hart, D.M. Minahan, J. Catal. 169 (1997) 438.
[3] W. Falter, C.H. Finkeldei, B. Jaeger, W. Keim, K.A.N. Verkerk, Stud. Surf. Sci. Catal. 119 (1998) 465.
[4] J.G. Nunan, R.G. Herman, K. Klier, J. Catal. 116 (1989) 222.
[5] M.T. Xu, M.J.L. Gines, A.M. Hilmen, B.L. Stephens, E. Iglesia, J. Catal. 171 (1997) 130.
[6] W. Keim, W. Falter, Catal. Lett. 3 (1989) 59.
[7] M. Roper, W. Keim, J. Seibring, DE Pat. 3,524,317(1987).
[8] M. Roper, W. Keim, DE Pat. 3,810,421(1989).
[9] C.H. Finkeldei, B. Jaeger, W. Keim, K.A.N. Verkerk, Prepr. Pap.-Am. Chem. Soc., Div. Fuel Chem. 41 (1996) 875.
[10] W. An, Y.Q. Niu, Z.H. Chen, J. Fuel. Chem. Technol. (China) 22 (1994) 63.
[11] J.W. Wang, Y.Q. Niu, Z.H. Chen, B. Zhong, S.Y. Peng, Nat. Gas Chem. Ind. (China) 22 (1997) 26.
[12] K.T. Jung, A.T. Bell, Catal. Lett. 1–2 (2002) 63.
[13] K. Pokrovski, K.T. Jung, A.T. Bell, Langmuir 17 (2001) 4297.
[14] K.L. Jung, A.T. Bell, J. Mol. Catal. 163 (2000) 27.
[15] M.J. Li, Z.C. Feng, G. Xiong, P.L. Ying, Q. Xin, C. Li, J. Phys. Chem. B 105 (2001) 8107.
[16] C. Schild, A. Wokaun, R.A. Koppel, A. Baiker, J. Catal. 130 (1991) 657.
[17] P.D.L. Mercera, J.G. van Ommen, E.B.M. Doesburg, A.J. Burggraaf, J.R.H. Ross, Appl. Catal. 57 (1990) 127.
[18] A. Sekkulic, K. Furic, J. Mater. Sci. Lett. 16 (1997) 260.
[19] T. Hirata, E. Asari, M. Kitajima, J. Solid State Chem. 110 (1994) 201.
[20] G. Stefanic, S. Music, B. Crzeta, S. Popovic, A. Sekulic, J. Phys. Chem. Solids 59 (1998) 879.
[21] E. Djurado, P. Bouvier, G. Lucazeau, J. Solid State Chem. 149 (2000) 399.
[22] R.C. Garvie, J. Phys. Chem. 69 (1965) 1238.
[23] P.D.L. Mercera, J.G. van Ommen, E.B.M. Doesburg, A.J. Burggraaf, J.R.H. Ross, Appl. Catal. 78 (1991) 79.
[24] R.L. Jones, D. Mess, Surf. Coat. Technol. 86 (1996) 94.
[25] K.J. Smith, C.W. Young, R.G. Herman, K. Klier, Ind. Eng. Chem. Res. 30 (1991) 61.
[26] N.B. Jackson, J.G. Ekerdt, J. Catal. 126 (1991) 31.